Laponite cascade assembly activated reversible multicolor luminescence supramolecular hydrogel with near-infrared emission

Rong Zhang, Yong Chen, Zhiyi Yu, Yu Liu

PII: \$1001-8417(25)00333-X

DOI: https://doi.org/10.1016/j.cclet.2025.111147

Reference: CCLET 111147

To appear in: Chinese Chemical Letters

Received date: 23 September 2024
Revised date: 12 March 2025
Accepted date: 26 March 2025



Please cite this article as: Rong Zhang, Yong Chen, Zhiyi Yu, Yu Liu, Laponite cascade assembly activated reversible multicolor luminescence supramolecular hydrogel with near-infrared emission, *Chinese Chemical Letters* (2025), doi: https://doi.org/10.1016/j.cclet.2025.111147

This is a PDF file of an article that has undergone enhancements after acceptance, such as the addition of a cover page and metadata, and formatting for readability, but it is not yet the definitive version of record. This version will undergo additional copyediting, typesetting and review before it is published in its final form, but we are providing this version to give early visibility of the article. Please note that, during the production process, errors may be discovered which could affect the content, and all legal disclaimers that apply to the journal pertain.

© 2025 Published by Elsevier B.V. on behalf of Chinese Chemical Society and Institute of Materia Medica, Chinese Academy of Medical Sciences.

### Chinese Chemical Letters

journal homepage: www.elsevier.com

#### Communication

# Laponite cascade assembly activated reversible multicolor luminescence supramolecular hydrogel with near-infrared emission

Rong Zhang, Yong Chen, Zhiyi Yu, Yu Liu\*

College of Chemistry, State Key Laboratory of Elemento-Organic Chemistry Nankai University, Tianjin 300071, China

#### ARTICLE INFO

#### **ABSTRACT**

Article history:
Received
Received in revised form
Accepted
Available online

Keywords: Supramolecular cascade system Multicolor luminescence Photo-responsiveness Cucurbituril

Dynamic anti-counterfeiting

Photo-responsive supramolecular assembly especially supramolecular hydrogels with tunable luminescence show a promising application potential in writable information recording and display materials. Herein, we report photo-responsive reversible multicolor supramolecular hydrogel with near-infrared emission, which is constructed by cucurbit[7]uril (CB[7]), cyanostilbene derivative (DAC) and Laponite XLG (LP) *via* supramolecular cascade assembly. Compared with the free guest molecule DAC, the confinement of macrocycle CB[7] achieve effective near-infrared fluorescence in the aqueous phase from scratch, and the subsequent cascade assembly with LP further restrict the molecular rotation of the DAC, which not only result in a substantial enhancement of the fluorescence intensity, but is also endowed with light-controlled fluorescence on/off both in the solution and hydrogel states. Further, 8-hydroxy-1,3,6-pyrenetrisulfonic acid trisodium salt (HPTS) is introduced in the cascade assembly to fabricated photo-controllable reversible multicolor luminescence supramolecular hydrogel between red and green induced by Förster resonance energy transfer, which is successfully employed in reversible multiple information encryption.

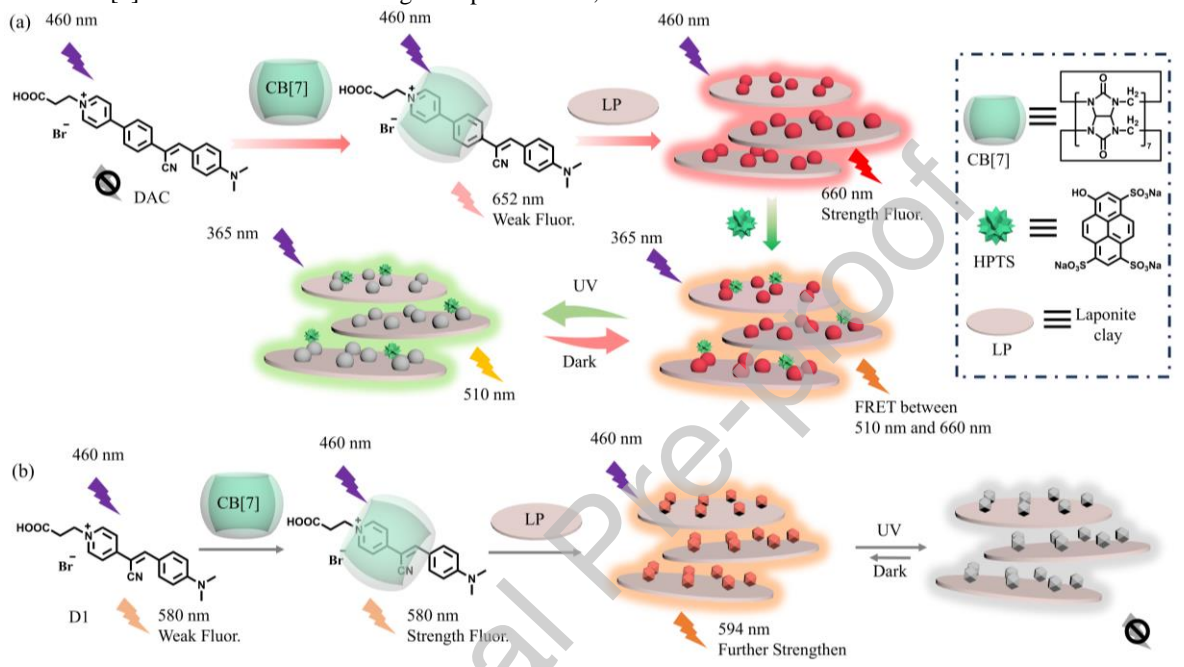
Smart materials with responsiveness to diverse stimuli have attracted great interest and extensive development in a variety of research fields [1-3], including information storage [4], biological diagnosis and treatment [5,6], intelligent sensing and detection [7]. Compared to other common external stimuli like pH [8,9], heat [10], and mechanical force [11-13], light stimuli-influenced systems have gained popularity among a wide range of researchers due to the non-invasiveness and high spatial-temporal resolution [14-16]. which greatly facilitates the construction of luminescent materials exhibiting luminescence on/off as well as tunable multicolor luminescence [17,18]. Typically, light-responsive luminescent systems mainly rely on molecular skeletons capable of photoisomerization and photoreactivity [19,20], such as azobenzene [21-24], diarylethylene [25-29], spiropyran [30,31], anthracene [32], indigoids [33], dihydropyrenes [34], and donoracceptor Stenhouse adducts [35], which exhibit high sensitivity and precise tunability, manifesting great potential in smart displays and multiple encryption [36-38]. Abe and coworkers reported a visible light-modulated fluorescence switch, in which a binaphthyl-bridged imidazole dimer with negative photochromic properties is directly as well as indirectly linked to the fluorophore naphthylimide, respectively, achieving fluorescence on/off driven by Förster resonance energy transfer through modulation of the colorless imidazole isomer under visible light irradiation or the colored form upon heating [39]. Yang group prepared spiropyranbased photomodulated liquid crystalline polymer (LCP) film with programmable glass transition temperature. In addition, the introduction of the aggregation-induced luminescence of cyanostyrene derivative (AIE-CSD) led to the LCP film exhibiting adjustable fluorescence between blue and red due to the fluorescence resonance energy transfer between spiropyran and AIE-CSD in different conformations induced by light irradiation, which were ultimately used for time-dependent information encryption [40]. Our group reported a photo-responsive supramolecular switch for photo-erased fluorescent inks, which was assembled by dialkylammonium-modified diarylethene derivative and dibenzo-24-crown-8 appended with [Ru(bpy)<sub>3</sub>]<sup>2+</sup> complex [41]. The luminescence of the supramolecular assembly turned on/off upon light irradiation of diverse wavelengths both in solution and in the solid state, which was successfully applied to reversible fluorescent ink.

In the research of photo-responsive supramolecular luminescence, supramolecular hydrogels constructed by cascade assembly have been rapidly developed because they not only have the semisolid property of three-dimensional networks which are used as an ideal matrix for constructing smart materials [42-44], but also have rich internal water environment and a porous architecture to load diverse functional components effectively [45], enabling diverse applications in dynamic information encryption [46,47], biomedicine, sensors and actuators [48,49]. However,

E-mail address: yuliu@nankai.edu.cn

<sup>\*</sup> Corresponding author.

multicolor reversible supramolecular luminescent hydrogels excited by short wavelengths, especially those with near-infrared emission, are still rare, to the best of our knowledge. Herein, we constructed a photo-controllable reversible near-infrared luminescent supramolecular cascade assembly based on the cucurbit[7]uril (CB[7]), cyanostilbene derivative (DAC) and anionic Laponite XLG (LP) (Scheme 1). The macrocycle host CB[7] encapsulated the guest molecule DAC with aggregationinduced luminescence properties, effectively realizing the confinement effect on DAC and thus inducing its near-infrared fluorescence at 652 nm in the aqueous phase. The binary assembly DACCB[7] was further co-assembled with LP through electrostatic interactions, which significantly enhanced the red Interestingly, the supramolecular fluorescence. system DACCB[7]/LP exhibited sensitive light responsiveness, whose red fluorescence gradually diminished under UV irradiation, then spontaneously and completely regained its original intensity by annealing in the dark. Moreover, a green fluorescent dye 8-hydroxy-1,3,6-pyrenetrisulfonic acid trisodium salt (HPTS) was introduced into the assembly, achieving the light-controlled multicolor luminescence between green and red both in solution and in LP-derived hydrogels. In addition, the luminescence changes of cyanoethylene derivatives with different substituents were investigated, demonstrating the generalized luminescence-enhancing effect of the cascade assembly strategy for a similar class of guest molecules. Benefiting from the light-controlled reversible luminescence property of DACCCB[7]/LP/HPTS assembly, it has been successfully applied to multiple information encryption with automatic erasure.



Scheme 1. Schematic illustration and molecular structures of unable luminescence supramolecular assembly (a) DACCB[7]/LP and (b) D1CB[7]/LP.

The guest molecule DAC, a cyanostilbene derivative modified with propionic acid at the nitrogen terminus, and reference molecules D1, and B1 with different substituents were synthesized according to the synthetic routes shown in Schemes S1-S3 (Supporting information), which was characterized by nuclear magnetic resonance (1H NMR, 13C NMR) and high-resolution mass spectrometry (HRMS), respectively (Figs. S1-S7 in Supporting information). The bonding behaviors between DAC and CB[7] were first studied by UV-vis absorption titration as well as NMR titration experiments. As shown in Fig. 1a, the characteristic absorption peak of DAC was centred at 438 nm, which gradually decreased and displayed a slight blueshift upon the gradual addition of CB[7], indicating the host-guest interaction between CB[7] and DAC. The association constant  $K_a$  of the inclusion complex was calculated to be  $1.27 \times 10^6$  L/mol based on the UV-vis absorption spectra vis the nonlinear curve-fitting method (Fig. S8 in Supporting information). In addition, the Job's plot showed the inflection point was at 0.5, demonstrating the stoichiometric ratio of DAC to CB[7] was 1:1 (Fig. S9 in Supporting information). According to the <sup>1</sup>H NMR titration experiments, the protons on the DAC pyridine ring upfield shifted after the addition of CB[7], while the protons of the alkyl chain groups of DAC downfield shifted, confirming the encapsulation of the CB[7] cavity to the DAC (Fig. 1b). In addition, the changes in morphology and particle size before and after the assembly were investigated. TEM images showed the morphology transformation of originally small-sized DAC particles into larger-sized nanospheres after the formation of the DAC\_CB[7] assembly (Fig. 1c, Fig. S10 in Supporting information), the DLS data (Fig. 1d and Fig. S11 in Supporting information) and SEM image (Fig. S12 in Supporting information) also corroborated that the effective diameter of the DAC\_CB[7] complex was about 100-200 nm, which likewise confirming the formation of the assemblies.

The luminescent behavior of DAC and their associated changes induced by assembly were then explored. As shown in Fig. 1e, DAC possessed no emission in an aqueous solution, however, the addition of CB[7] caused the NIR fluorescence at 652 nm with an excitation wavelength of 460 nm (Fig. S13 in Supporting information). Additionally, the enhancement in NIR fluorescence intensity of DAC was observed by gradually increasing the proportion of undesirable solvent dichloromethane for DAC (Fig. S14 in Supporting information), confirming that the assemblyinduced NIR luminescence originates from the intrinsic aggregation-induced luminescence property of DAC. These results demonstrated that the hydrophobic cavity of the macrocycle CB[7] effectively restricted the molecular motions of DAC thereby inducing its intrinsic luminescence to be visible in the aqueous phase. Compared to other macrocycles including the larger cavity cucurbit[8]uril (CB[8]), the negatively charged sulfobutylether- $\beta$ -cyclodextrin (SBE- $\beta$ -CD), and the amphiphilic calix[4]arene (SC4A8) (Fig. S15 in Supporting information), CB[7] with a more suitable cavity size was optimal for boosting the luminescence of DAC in terms of the luminescence intensity and the more red-shifted fluorescence.



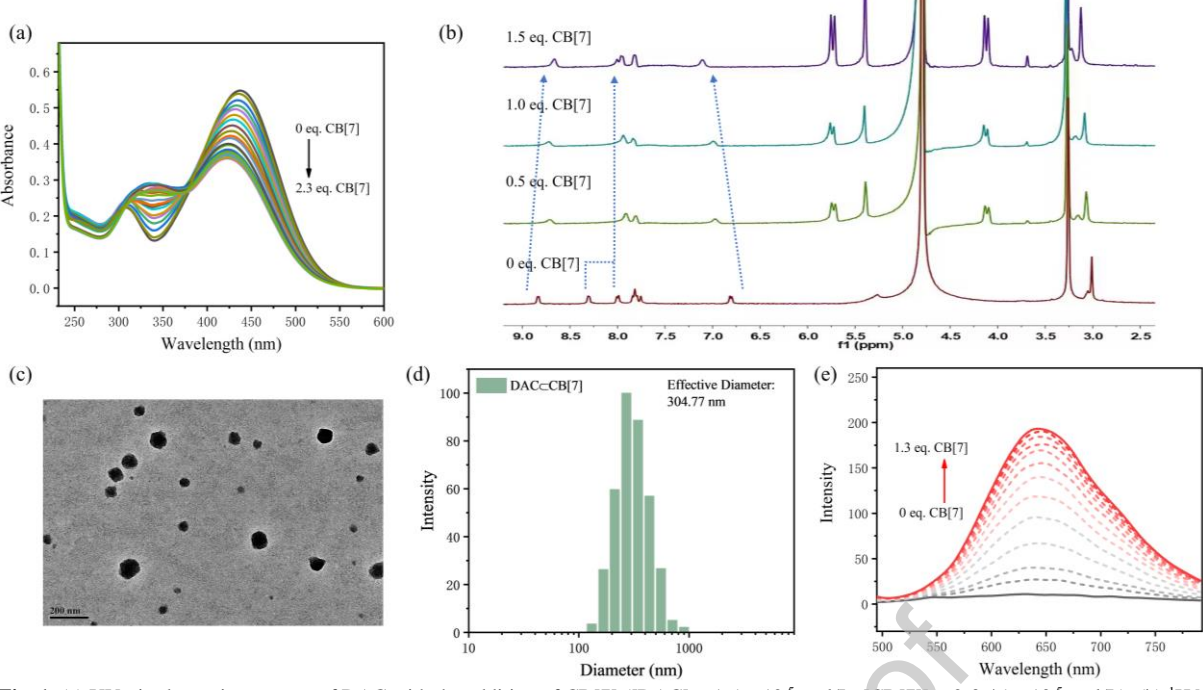


Fig. 1. (a) UV-vis absorption spectra of DAC with the addition of CB[7] ([DAC] =  $1.5 \times 10^{-5}$  mol/L, [CB[7]] =  $0-3.45 \times 10^{-5}$  mol/L). (b) <sup>1</sup>H NMR spectra of DAC with the addition of 0, 0.5, 1.0, 1.5 equiv. CB[7] (400 MHz, D<sub>2</sub>O/CD<sub>3</sub>OD = 8:2, 25 °C, [DAC] =  $1.0 \times 10^{-3}$  mol/L, [CB[7]] =  $0-1.5 \times 10^{-3}$  mol/L). (c) TEM images of DAC CB[7] ([DAC] =  $2 \times 10^{-5}$  mol/L, [CB[7]] =  $2 \times 10^{-5}$  mol/L). (d) DLS results of DAC CB[7]. (e) Fluorescence spectra of DAC with the addition of CB[7] ([DAC] =  $2.0 \times 10^{-5}$  mol/L, [CB[7]] =  $0-2.6 \times 10^{-5}$  mol/L).

To further enhance the luminescence intensity, LP with abundant negative charges was chosen to co-assemble with the supramolecular assembly DACCB[7]. As observed in the UV vis absorption spectra (Fig. S16 in Supporting information), the major absorption peak of the supramolecular cascade assembly DACCCB[7]/LP was red-shifted to 476 nm after the addition of LP. In addition, the fluorescence was slightly red-shifted upon the addition of LP to the DACCB[7], and the fluorescence intensity at 660 nm was enhanced by a factor of 10 when 2.5 mg/mL of LP was added (Fig. 2a), indicating that the negatively-charged-rich lamellar LP facilitated the further restriction of molecular motions of DAC to achieve a significant enhancement of fluorescence. And the excitation-dependent emission maps of DACCB[7]/LP indicated the fluorescence emission was centred at around 660 nm, with the optimal excitation being 460 nm (Fig. 2b). In contrast, the fluorescence intensity was only enhanced by 2 or 3 times when other negatively charged compounds such as SBE-\beta-CD and SC4A8 were used for co-assembly with DACCCB[7] complex (Fig. S17 in Supporting information). In addition, a comparison of the fluorescence spectra of DACCB[7]/LP and DAC/LP showed enhanced fluorescence intensity in the presence of CB[7] (Fig. S18 in Supporting information), illustrating the necessity of CB[7] and LP participation in cascade assembly for enhanced fluorescence emission. The fluorescence lifetime of the ternary supramolecular complex DAC⊂CB[7]/LP was measured to be 2.27 ns, which was a negligible change compared to that of 2.86 ns for DACCB[7] and 6.20 ns for DAC (Fig. 2c). The photoluminescence quantum yield of DAC⊂CB[7]/LP was calculated to be 3.28%, which was significantly higher than that of monomer DAC (0.08%) and supramolecular inclusion complex DAC⊂CB[7] (1.07%) (Fig. 2d and Fig. S19 in Supporting information).

Interestingly, the cascade assembly DACCB[7]/LP exhibited light responsiveness, whose NIR fluorescence gradually quenched under UV irradiation within 30 s (Fig. 2e) and reversed after keeping in the dark for 6 h, thus realizing dark/UV regulated fluorescence on/off. The photo-switching performance of the ternary supramolecular complex DACCB[7]/LP presented excellent fatigue resistance and could be cycled more than five

times under alternating UV light irradiation and dark treatment without significant attenuation (Fig. 2f). Reversible recovery of quenched fluorescence could also be achieved by keeping it at 60 °C for 30 min (Fig. S20 in Supporting information). It was hypothesized that the reason for the photo-switching property may be the photoinduced cis-trans isomerism of DAC, where the trans-DAC was aggregation-induced luminescent, while the cis-DAC induced by UV irradiation exhibited aggregation-induced quenching [50,51], followed by annealing in the dark that transformed the cis DAC to the trans form once again thereby turning on the luminescence to achieve the reversible supramolecular light switch [52]. The major absorption peak at 468 nm of the ternary supramolecular complex DACCCB[7]/LP in aqueous solution blue-shifted and slightly increased under UV light irradiation (Fig. S21 in Supporting information), and the <sup>1</sup>H NMR spectra showed chemical shift changes of DAC after UV illumination (Fig. S22 in Supporting information), indicating that UV irradiation-induced the isomerism of DAC leading to fluorescence quenching. Since LP has the characteristic of spontaneous coagulation, we subsequently increased the concentration of LP to 25mg/mL to obtain supramolecular hydrogel and explored the rheological properties [53]. The frequency sweep tests of the hydrogel DAC $\subset$ CB[7]/LP at  $\omega$  = 0.01-100 rad/s and strain ( $\gamma$ ) = 1% were firstly carried out. In the range of frequency ω from 0.01 to 100 rad/s, the storage modulus (G') was always greater than the loss modulus (G''), which indicated that the supramolecular hydrogel remained stable under the condition of 1% strain. According to the strain sweep tests at y = 0.01-100% with  $\omega$  = 6.28 rad/s, hydrogel DAC $\subset$ CB[7]/LP underwent the transition from gel to sol under high strain. Continuous step strain tests of hydrogel DAC⊂CB[7]/LP showed G' decreased rapidly under high strain ( $\gamma = 100\%$ ,  $\omega = 6.28$  rad/s) for 100 s, indicating that the structure of the hydrogel was destroyed. When the strain decreased to 0.01%, G' returned to the initial state, suggesting that the structure of the hydrogel was restored. The transformation of the gel-sol could be repeated several times under alternating strain, confirming that the supramolecular hydrogel DAC⊂CB[7]/LP possessed excellent

self-healing performance (Fig. S23 in Supporting information). The luminescent behavior of the supramolecular hydrogel was then investigated. The fluorescence intensity of supramolecular hydrogel DACCCB[7]/LP was significantly higher than that of both the free guest DAC solution and DACCCB[7] solution. At the same time, the hydrogel still exhibited sensitive light response

performance. Upon UV light irradiation in 30 s, the fluorescence intensity of the hydrogel DAC $\subset$ CB[7]/LP turned off, while the red fluorescence turned on in the dark for 6 h. The light switching progress could be repeated more than five times without obvious fatigue (Fig. S24 in Supporting information).

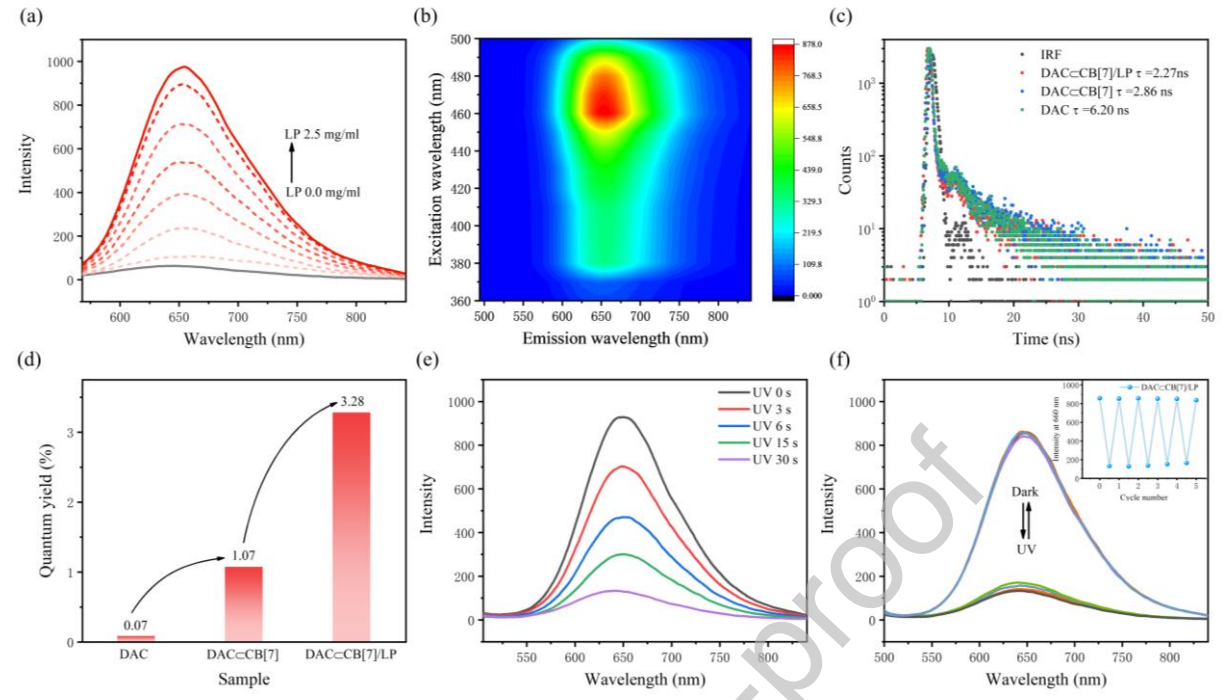


Fig. 2. (a) Fluorescence spectra of DAC $\subset$ CB[7] with the gradual addition of LP from 0-2.5 mg/mL ([DAC] =  $2\times10^{-5}$  mol/L, [CB[7]] =  $2\times10^{-5}$  mol/L). (b) Fluorescence excitation mapping of the DAC $\subset$ CB[7]/LP. (c) Photoluminescence lifetime of DAC, DAC $\subset$ CB[7], and DAC $\subset$ CB[7]/LP, respectively with the instrument response function (IRF) ([DAC] =  $2.0\times10^{-5}$  mol/L, [CB[7]] =  $2.0\times10^{-5}$  mol/L, [LP] = 2.5 mg/ml). (d)The fluorescence quantum yields of DAC, DAC $\subset$ CB[7]/LP ([DAC] =  $2.0\times10^{-6}$  mol/L, [CB[7]] =  $2.0\times10^{-6}$  mol/L, [LP] = 0.25 mg/mL). (e) Fluorescence spectra of DAC $\subset$ CB[7]/LP upon UV irradiation in 30 s. (f) Fluorescence spectra of DAC $\subset$ CB[7]/LP under alternating UV irradiation and darkness. Insert: the corresponding changes of fluorescence of DAC $\subset$ CB[7]/LP at 660 nm ([DAC] =  $2\times10^{-5}$  mol/L, [CB[7]] =  $2\times10^{-5}$  mol/L, [LP] = 2.5 mg/mL).

In addition, B1 and D1 were employed as reference molecules to investigate the luminescence changes in the cascade supramolecular complex of structurally similar cyanostilbene derivatives. For the guest molecule D1, which emitted a weak orange-red fluorescence at 580 nm in aqueous solution but no emission in the solid state due to the ACQ effect. The fluorescence intensity of D1 was enhanced by the addition of CB[7], however, when CB[8] with a larger cavity size was added, the fluorescence emission red-shifted (Fig. S25 in Supporting information). After further introduction of LP, the fluorescence enhancement of the ternary supramolecular complex D1 CB[7]/LP was significantly higher than that of D1⊂CB[8]/LP (Fig. 3a, Fig. S26 in Supporting information), indicating that CB[7] with a more matching cavity size was more conducive to constructing a supramolecular system with strengthen fluorescence intensity for D1. In addition, the excitation-dependent fluorescence mapping of D1CB[7]/LP confirmed the fluorescence emission was centred at around 660 nm under the optimal excitation wavelength of 460 nm (Fig. 3b). Similarly, B1 with blue-green fluorescence excited by 365 nm also exhibited fluorescence enhancement with a slight blue shift induced by CB[7] encapsulation and a red shift upon the addition of CB[8] (Fig. 3d, Fig. S27 in Supporting information). Subsequently, LP was introduced to form the ternary supramolecular complex B1CB[7]/LP, which exhibited stronger blue fluorescence at 470 rather than B1⊂CB[8]/LP (Fig. 3c, Fig. S28 in Supporting information). The photoluminescence quantum yield results showed a quantum yield of 19.62% for D1⊂CB[7]/LP and 60.14% for B1⊂CB[8]/LP (Fig. S29 in Supporting information). All the results illustrated the universality of the cascade assembly strategy by CB[7] and LP for fluorescence

enhancement of this class of structurally similar molecules. Moreover, the bonding behavior of D1 and B1 to CB[7] was studied separately. Job's plot revealed that the inflection point of inclusion complex D1 CB[7] was at 0.5 (Fig. S30 in Supporting information), indicating that the bonding ratio of CB[7] to D1 was stoichiometric 1:1. And in the UV-vis absorption spectra, the characteristic absorption peak at 502 nm of D1 gradually decreased and faintly red-shifted with the gradual addition of CB[7], the association constant  $K_a$  for CB[7] to D1 were calculated to be  $8.66 \times 10^6$  L/mol by nonlinear curve fitting (Fig. S30). According to the <sup>1</sup>H NMR spectra, the upfield shift of protons on the pyridine of D1 was observed after the addition of CB[7], which indicated that the pyridine portion of D1 was encapsulated within the CB[7] cavity (Fig. S31 in Supporting information). On the other hand, Job's plot showed the inflection point of inclusion complex B1⊂CB[7] also occurred at 0.5, proving the bonding ratio between B1 and CB[7] was stoichiometric 1:1 (Fig. S32 in Supporting information). The major absorption peak of B1 decreased and red-shifted upon the addition of CB[7], and the association constant  $K_a$  of CB[7] to B1 was calculated to be 1.42 × 10<sup>6</sup> L/mol from nonlinear curve fitting based on the change in UV-vis absorption at 500 nm (Fig. S32 in Supporting information).

The photo-responsive behaviors of the ternary supramolecular complex D1 $\subset$ CB[7]/LP and B1 $\subset$ CB[7]/LP were then explored. As anticipated, the initial orange-red fluorescence at 580 nm of D1 $\subset$ CB[7]/LP gradually decreased under UV irradiation (Fig. S33 in Supporting information), however, the fluorescence intensity recovered incompletely when placed in the dark for 6 h (Fig. 3e). For another ternary supramolecular complex B1 $\subset$ CB[7]/LP, UV

irradiation resulted in almost complete quenching of the fluorescence at 470 nm without any restoration in the dark (Fig. 3f, Fig. S33), demonstrating although the cyanostilbene derivatives D1 and B1 were responsive to UV light, only DAC

exhibited excellent reversibility in the photo-switching performance. Considering the practical application scenarios, the ternary supramolecular complex DAC CB[7]/LP of superior light responsiveness was chosen for subsequent luminescence studies.

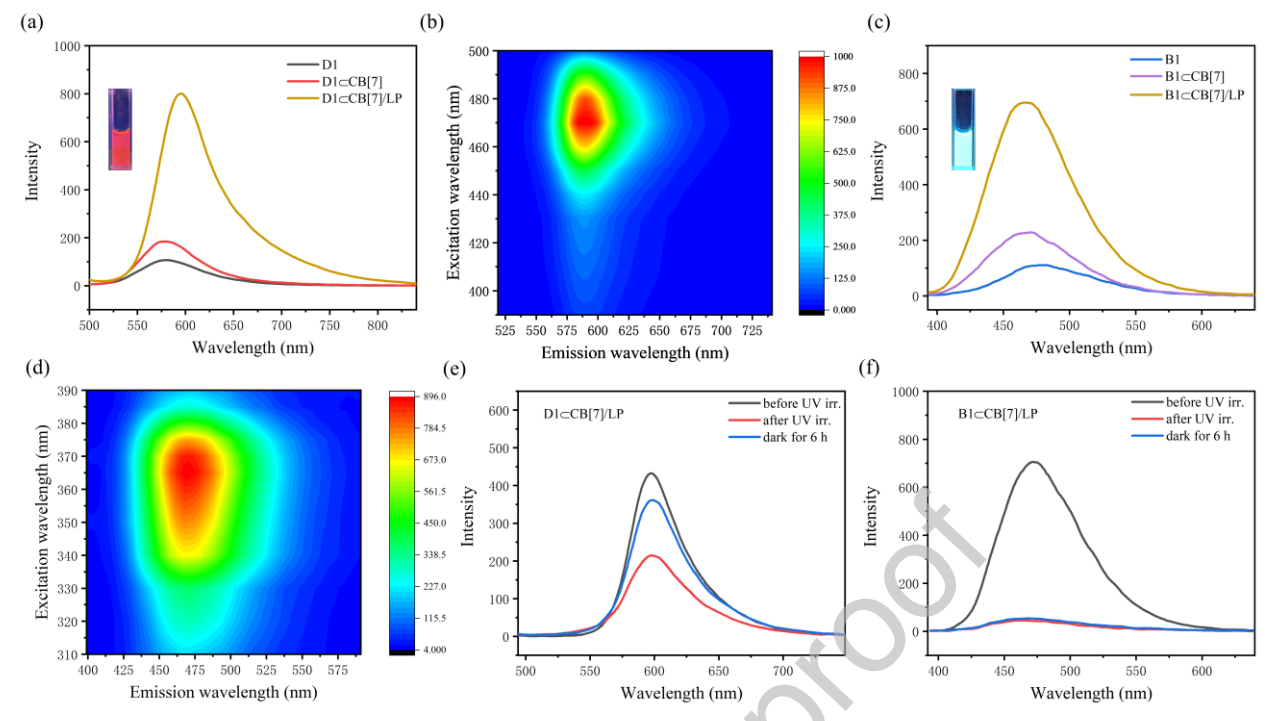


Fig. 3. (a) Fluorescence spectra of D1, D1 $\subset$ CB[7] and D1 $\subset$ CB[7]/LP ([D1] = 2 × 10<sup>-5</sup> mol/L, [CB[7]] = 2 × 10<sup>-5</sup> mol/L, [LP] = 2.5 mg/mL). (b) Fluorescence excitation mapping of the D1 $\subset$ CB[7]/LP. (c) Fluorescence spectra of B1, B1 $\subset$ CB[7] and B1 $\subset$ CB[7]/LP ([B1] = 2 × 10<sup>-5</sup> mol/L, [CB[7]] = 2 × 10<sup>-5</sup> mol/L, [LP] = 2.5 mg/mL). (d) Fluorescence excitation mapping of the B1 $\subset$ CB[7]/LP. (e) Fluorescence spectra of D1 $\subset$ CB[7]/LP upon UV irradiation and in the dark ([D1] = 2 × 10<sup>-5</sup> mol/L, [CB[7]] = 2 × 10<sup>-5</sup> mol/L, [LP] = 2.5 mg/mL). (f) Fluorescence spectra of B1 $\subset$ CB[7]/LP upon UV irradiation and in the dark ([B1] = 2 × 10<sup>-5</sup> mol/L, [CB[7]] = 2 × 10<sup>-5</sup> mol/L, [LP] = 2.5 mg/mL).

Benefiting from the remarkable light-switching performance of the ternary supramolecular complex DACCB[7]/LP, it was thus promising for further construction of a light-controlled multicolor luminescence system with other fluorophores. A distinct and stable fluorescent dye HPTS was introduced in DACCCB[7]/LP to construct a photo-modulated multicolor luminescence between green and red. As shown in Fig. 4a, the emission spectrum of the HPTS greatly overlapped with the absorption spectrum of the DACCCB[7]/LP, which was the basis for realizing the Förster resonance energy transfer (FRET) between HPTS and DACCB[7]/LP. As a result, the fluorescence intensity of HPTS at 510 nm gradually decreased with the addition of DAC in the presence of CB[7] and LP when excited at 365 nm based on the excitation spectra of HPTS (Fig. S34 in Supporting information), while the fluorescence at 660 nm attributed to DACCCB[7]/LP was subsequently enhanced, indicating the occurrence of FRET from HPTS to DACCB[7]/LP (Fig. 4b). The 1931 CIE chromaticity diagrams as well as photographs under a UV portable lamp tracked the fluorescence color change during the FRET process, which went through green, yellow, orange to red with increasing the proportion of DACCB[7]/LP cascade assembly to the HPTS (Fig. 4c). The energy transfer efficiency from HPTS to the assembly DACCCB[7]/LP was calculated to be 90.77% when the concentration of the added assembly was  $2 \times 10^{-5}$  mol/L. The rheological experiments of hydrogel DAC⊂CB[7]/LP/HPTS showed HPTS as a small amount of dopant has no significant effect on the stability and mechanical properties of hydrogel (Fig. Supporting information). In addition, S35 DACCB[7]/LP/HPTS system still exhibited good light regulatability, the UV light irradiation transformed the system that originally emitted red fluorescence into green due to UV-driven fluorescence off of the DACCB[7]/LP (Fig. 4d). Then the fluorescence gradually reversed in the dark for about 6 hours (Fig. S36 in Supporting information), which could be reversibly cycled more than five times without significant fatigue under alternating UV irradiation and darkness (Figs. 4e and 4f).

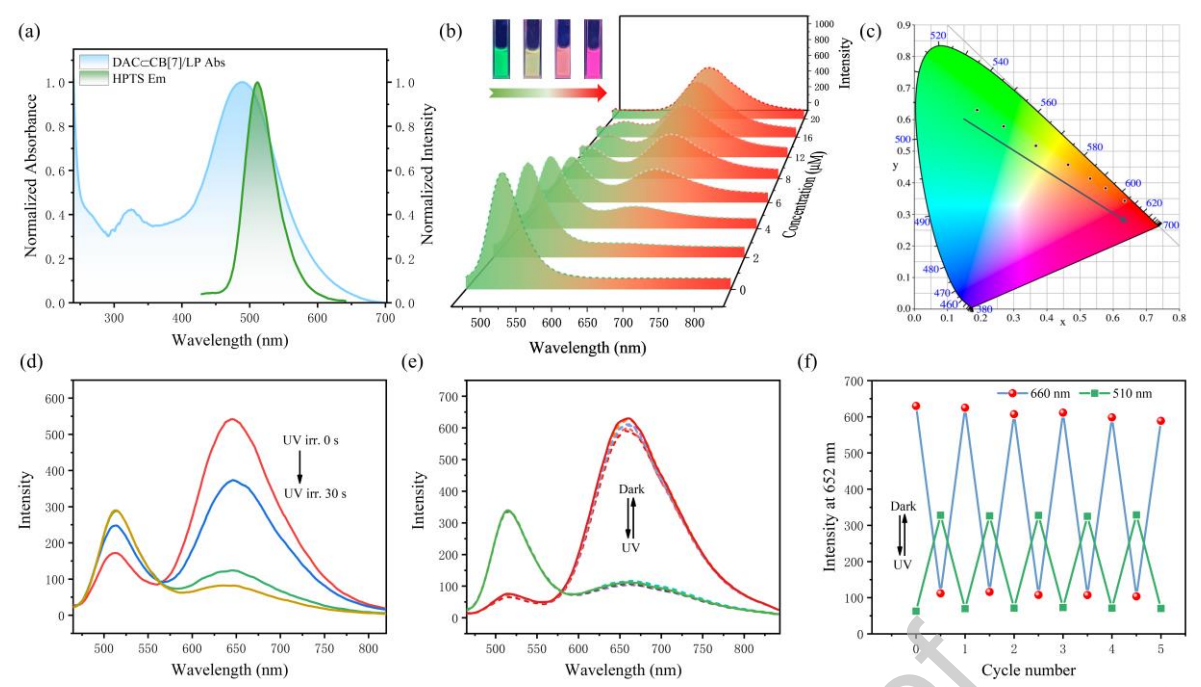


Fig. 4. (a) UV-Vis absorption spectra of DAC $\subset$ CB[7]/LP and fluorescence spectra of HPTS ([DAC] =  $2 \times 10^5$  mol/L, [CB[7]] =  $2 \times 10^5$  mol/L, [LP] = 2.5 mg/mL, [HPTS] =  $2 \times 10^7$  mol/L). (b) The fluorescence changes of HPTS upon gradual addition of the DAC in the presence of CB[7] and LP. Insert: photographs under a UV portable lamp of DAC $\subset$ CB[7]/LP/HPTS complex ([DAC] =  $0-2 \times 10^5$  mol/L, [CB[7]] =  $2 \times 10^5$  mol/L, [LP] = 2.5 mg/mL, [HPTS] =  $2 \times 10^7$  mol/L). (c) The 1931 CIE chromaticity diagrams of HPTS with the gradual addition of the DAC $\subset$ CB[7]/LP, (d) Fluorescence spectra of DAC $\subset$ CB[7]/LP/HPTS under UV irradiation in 30 s. (e) Fluorescence spectra of DAC $\subset$ CB[7]/LP/HPTS under alternating UV irradiation and darkness. (f) Changes in the emission intensity at 660 nm and 510 nm according to (e) ([DAC] =  $2 \times 10^5$  mol/L, [CB[7]] =  $2 \times 10^5$  mol/L, [LP] = 2.5 mg/mL, [HPTS] =  $2 \times 10^7$  mol/L).

Taking advantage of the remarkable light-tunable reversible multicolor luminescence properties, quaternary supramolecular complex DACCB[7]/LP/HPTS was capable of exploiting their full potential in multiple information encryption. Since the supramolecular complex DACCB[7]/LP/HPTS presented red fluorescence under darkness and produced a contrasting green fluorescence upon UV light irradiation, the change of information was driven by the stimulation of light thereby realizing multiple encryptions. As shown in the schematic diagram for the display of information encryption in Fig. 5a, the aqueous solution of DACCCB[7]/LP supramolecular complex and DACCCB[7]/LP/HPTS was dropped into the corresponding holes in the 96-well plate, depicting the Arabic number "888" with red luminescence as the initial primary information. Then after the irradiation with a UV lamp for 30 s, the red fluorescence of DACCB[7]/LP quenched and that of DACCB[7]/LP/HPTS changed from red to green at the same time, which resulted in the secondary information of number group "502" displaying as the correct message. Secondary information could also spontaneously revert to primary information when the UV light source was turned off and the 96-well plate was in the dark for several hours, thus achieving erasable and automatic recovering information encryption. The photograph under the UV lamp well confirmed the light-controllable multiple information display and erasure (Fig. 5b). Furthermore, the Morse code that represented various information through different permutations was also been employed for multiple information encryption. Utilizing two supramolecular complexes DACCB[7]/LP and DACCCB[7]/LP/HPTS with red fluorescence to fill specific positions in the 96-well plate, obtaining primary information the letter combination "MAX"

Subsequently, the information transformed into a green luminescent Moss code representing the correct information "TEA" after being irradiated with UV light, which reversibly returned to the initial red code containing information "MAX" after keeping in the dark for 6 hours (Fig. 5d).

Considering the limitation of highly fluid aqueous solution in the application environments where fixed shapes were required, anti-counterfeit applications based on LP hydrogels with spontaneous rapid coagulation and excellent self-healing properties have been further explored. The supramolecular hydrogel was prepared by DACCB[7] and negatively charged LP, i.e., the concentration of LP was increased to 25 mg/mL and the aqueous solution was poured into the mold and left for 3 h. As shown in the schematic diagram in Fig. 5e, the supramolecular hydrogel was covered with a homemade mask engraved with letters, and the UV light was irradiated to the exposed portion of the hydrogel so as to photolithographically engrave the letter "N", whereas the letter "N" gradually disappeared by removing the external light source and keeping it out of the light. The supramolecular hydrogel was able to be reused in information encryption by utilizing the characteristics of writing upon UV light irradiation and self-erasure in the dark. As a result, the green luminescent capital letters "N", "K", and "U" successively displayed when the supramolecular hydrogel was covered with masks with different skeletonized letters after a UV-darkness cycle according to the photographs captured under a UV portable light (Fig. 5f). Successful writing and erasing of information in both solution and hydrogel states indicated that the assembly system was capable of anti-counterfeiting in different environments, which was conducive to further potential in intelligent response materials.

# (a) UV Dark 000 ... ... ... DACCCB[7]/LP/HPTS ● DAC⊂CB[7]/LP (b) (c) (d) (e) cover masl UV irr. 30 s Dark 6 h DACCEB[7]/LP/HPTS Hydrogel (f)

Fig. 5. (a) Schematic diagram and (b) photographs of UV-induced display of encrypted numbers and darkness-induced information erasure based on supramolecular cascade assembly DAC $\subset$ CB[7]/LP/HPTS and DAC $\subset$ CB[7]/LP (DAC =  $2 \times 10^{-5}$  mol/L, CB[7] =  $2 \times 10^{-5}$  mol/L, LP = 2.5 mg/mL, HPTS =  $2 \times 10^{-7}$  mol/L). (c) Schematic illustration and (d) photographs of reversible changes of Morse code under alternating UV light irradiation and darkness based on supramolecular cascade assembly DAC $\subset$ CB[7]/LP/HPTS and DAC $\subset$ CB[7]/LP (DAC =  $2 \times 10^{-5}$  mol/L, CB[7] =  $2 \times 10^{-5}$  mol/L, LP = 2.5 mg/mL, HPTS =  $2 \times 10^{-7}$  mol/L). (e) Schematic diagram and (f) images under UV lamp of the construction of writable and self-erasing DAC $\subset$ CB[7]/LP/HPTS supramolecular hydrogel (DAC =  $2 \times 10^{-5}$  mol/L, CB[7] =  $2 \times 10^{-5}$  mol/L, LP = 2.5 mg/mL, HPTS =  $2 \times 10^{-7}$  mol/L).

In conclusion, we constructed controllable reversible multicolor supramolecular luminescent hydrogel via the guest DAC with aggregation-induced luminescence properties, macrocycle host CB[7], abundantly negatively charged LP, and green fluorescent dye HPTS. Firstly, the DACCB[7] assembly was constructed by the stronger bonding ability of CB[7] to DAC, which produced a red fluorescence at 652 nm due to the macrocycle confinement effect of CB[7] to the guest DAC. Subsequently, LP whose abundant negative charge and lamellar structure favor trapping and restricting the molecular motion of DAC was chosen to further construct the secondary assembly DACCB[7]/LP, showing significantly enhanced and weakly red-shifted luminescence at 660 nm. It was surprising that the cascade assemblies were found to be light modulation, whose red fluorescence was quenched under UV illumination and turned on spontaneously in the dark. Furthermore, HPTS was introduced to co-assembly with DACCB[7]/LP, producing multicolor reversible fluorescence between green and red upon alternating UV irradiation and darkness. The DACCB[7]/LP/HPTS supramolecular assembly was successfully applied in writeable and self-erasing information encryption, thus the cascade assembly supramolecular strategy provided a new approach for multiple anti-counterfeiting applications.

### **Declaration of competing interest**

The authors report no declarations of interest.

### Acknowledgments

We thank National Natural Science Foundation of China (NNSFC) (22131008) and the Haihe Laboratory of Sustainable Chemical Transformations for financial support.

#### References

[1] C. Kaspar, B. J. Ravoo, W. G. van der Wiel, S. V. Wegner, W. H. P. Pernice, Nature 594 (2021) 345-355.

[2] W. T. Xu, X. Li, P. C. Wu, et al., Angew. Chem. Int. Ed. 63 (2024) e202319502:

[3] Q. K. Qi, S. Q. Huang, X. G. Liu, I. Aprahamian, J. Am. Chem. Soc. 146 (2024) 6471-6475.

[4] W. W. Xu, Y. Chen, X. F. Xu, Y. Liu, Small. 20 (2024) 2311087.[5] Y. Chen, L. B. Li, L. S. Gong, T. Y. Zhou, J. B. Liu, Adv. Funct. Mater. 29 (2019) 1806945.

[6] W. Szymanski, J. M. Beierle, H. A. V. Kistemaker, W. A. Velema, B. L. Feringa, Chem. Rev. 113 (2013) 6114-6178.

[7] M. L. Lian, J. Zhao, D. Zhang, et al., Angew. Chem. Int. Ed. 63 (2024) e202401228.

[8] Y. L. Zhu, Y. G. Tang, P. Miao, Langmuir. 40 (2023) 1130-1136. [9] Z. Liu, H. Chen, M. Tian, et al., Aggregate (2024) e627.

[10] X. L. Zhou, X. Zhao, X. Bai, Q. W. Cheng, Y. Liu, Adv. Funct. Mater. 34 (2024) 2400898.

- [11] J. F. Liu, D. K. Ma, C. Z. Qi, D. P. Yang, S. M. Huang, ACS Appl. Mater. Inter. 16 (2024) 2740-2750.
- [12] Y. Zhang, Y. Chen, J. Q. Li, S. E. Liu, Y. Liu, Adv. Sci. 11 (2024) 2307777.
- [13] Y. Yin, Q. C. Guan, Z. Chen, et al., Sci. Adv. 10 (2024) eadk5444. [14] R. Lan, J. Bao, Z. Li, et al., Angew. Chem. Int. Ed. 61 (2022) e202213915.
- [15] R. Zhang, Y. Chen, L. Chen, Y. Zhang, Y. Liu, Adv. Opt. Mater. 11 (2023) 2300101.
- [16] H.J. Wang, H.Y. Zhang, W.W. Xing, et al., Chin. Chem. Lett. 33 (2022) 4033-4036.
- [17] L. Fei, W. D. Yu, Z. H. Wu, et al., Angew. Chem. Int. Ed. 61 (2022) e202212483.
- [18] Y. Ma, J. D. Shen, J. F. Zhao, et al., Angew. Chem. Int. Ed. 61 (2022) e202202655.
- [19] D. Bléger, S. Hecht, Angew. Chem. Int. Ed. 54 (2015) 11338-11349.
- [20] S. Y. Lin, K. G. Gutierrez-Cuevas, X. F. Zhang, J. B. Guo, Q. Li, Adv. Funct. Mater. 31 (2021) 2007957.
- [21] Y. Z. Liu, H. L. Wang, P. R. Liu, et al., Angew. Chem. Int. Ed. 60 (2021) 5766-5770.
- [22] L. N. Lameijer, S. Budzak, N. A. Simeth, et al., Angew. Chem. Int. Ed. 59 (2020) 21663-21670.
- [23] H. M. D. Bandara, S. C. Burdette, Chem. Soc. Rev. 41 (2012) 1809-1825.
- [24] P. Lentes, E. Stadler, F. Röhricht, et al., J. Am. Chem. Soc. 141 (2019) 13592-13600.
- [25] M. Irie, T. Fulcaminato, K. Matsuda, S. Kobatake, Chem. Rev. 114 (2014) 12174-12277.
- [26] T. Fukaminato, T. Hirose, T. Doi, et al., J. Am. Chem. Soc. 136 (2014) 17145-17154.
- [27] R. Kashihara, M. Morimoto, S. Ito, H. Miyasaka, M. Irie, J. Am. Chem. Soc. 139 (2017) 16498-16501
- [28] H. C. Xi, Z. P. Zhang, W. W. Zhang, et al., J. Am. Chem. Soc 141 (2019) 18467-18474.
- [29] C. H. Wang, Y. M. Zhang, H. R. Li, et al., Chin. Chem. Lett. 33 (2022) 2447-2450.
- [30] L. Kortekaas, W. R. Browne, Chem. Soc. Rev. 48 (2019) 3406-
- [31] R. Klajn, Chem. Soc. Rev. 43 (2014) 148-184.
- [32] J. H. Huang, Y. Jiang, Q. Y. Chen, H. Xie, S. B. Zhou, Nat. Commun. 14 (2023) 7131.
- [33] C. Y. Huang, A. Bonasera, L. Hristov, et al., J. Am. Chem. Soc. 139 (2017) 15205-15211.
- [34] K. Klaue, W. J. Han, P. Liesfled, et al., J. Am. Chem. Soc. 142 (2020) 11857-11864.
- [35] L. Fang, Z. W. Lin, Y. Zhang, et al., Angew. Chem. Int. Ed. 63 (2024) e202402349.
- [36] Y. L. Huang, H. K. Bisoyi, S. Huang, et al., Angew. Chem. Int. Ed. 60 (2021) 11247-11251.
- [37] R. Zhang, Y. Chen, Y. Liu, Angew. Chem. Int. Ed. 62 (2023) e202315749.
- [38] W. C. Zhong, L. Shang, Chem. Sci. 15 (2024) 6218-6228.
- [39] K. Mutoh, N. Miyashita, K. Arai, J. Abe, J. Am. Chem. Soc. 141 (2019) 5650-5654.
- [40] J. Y. Zhang, C. J. Song, S. N. Zhang, et al., Adv. Funct. Mater. 34 (2024) 2400030.
- [41] H. Wu, Y. Chen, Y. Liu, Adv. Mater. 29 (2017) 1605271.
- [42] W. L. Zhou, Y. G. Wu, S. W. Wang, et al., Biosens. Bioelectron. 258 (2024) 116343.
- [43] S. E. Liu, Y. Zhang, J. Q. Li, et al., ACS Appl. Mater. Inter. 16 (2024) 5149-5157.
- [44] Z. Li, X. F. Ji, H. L. Xie, B. Z. Tang, Adv. Mater. 33 (2021) 2100021
- [45] H. Liu, S. X. Wei, H. Y. Qiu, et al., Adv. Funct. Mater. 32 (2022) 2108830.
- [46] Y. Sun, X. X. Le, H. Shang, et al., Adv. Mater. 36 (2024) 2401589.

- [47] B. Y. Wu, M. Q. Si, L. Q. Hua, et al., Adv. Mater. 36 (2024) 2401659.
- [48] G. M. Y. Su, N. Wang, Y. K. Liu, et al., Adv Mater. 36 (2024) 2400085.
- [49] H. L. Yang, S. N. Li, J. X. Zheng, et al., Adv. Mater. 35 (2023) 2301300.
- [50] P. Y. Xing, H. Z. Chen, L. Y. Bai, Y. L. Zhao, Chem. Commun. 51 (2015) 9309-9312.
- [51] L. L. Zhu, X. Li, Q. Zhang, X. Ma, et al., J. Am. Chem. Soc. 135 (2013) 5175-5182.
- [52] Q. H. Cheng, Z. Z. Cao, A. Y. Hao, Y. L. Zhao, P. Y. Xing, ACS Appl. Mater. Inter. 12 (2020) 15491-15499.
- [53] G. X. Liu, Y.M. Zhang, X. F. Xu, L. Zhang, Y. Liu, Adv. Optical Mater. 5 (2017) 1700149.

### **Graphical Abstract**

Laponite cascade assembly activated reversible multicolor luminescence supramolecular hydrogel with nearinfrared emission

Rong Zhang, Yong Chen, Zhiyi Yu, Yu Liu\*

College of Chemistry, State Key Laboratory of Elemento-Organic Chemistry, Nankai University, Tianjin 300071, China

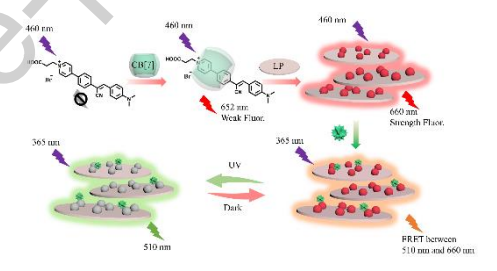


Photo-controllable multicolor supramolecular hydrogel switch was constructed by macrocycle cucurbit[7]uril, cyanostilbene derivative, Laponite and green fluorescent dye cascade assembly, exhibiting reversible multicolor luminescence between red and green for successful application in writable and self-erasing dynamic anti-counterfeiting.

#### **Declaration of competing interest**

The authors report no declarations of interest.

E-mail address: yuliu@nankai.edu.cn

<sup>\*</sup> Corresponding author.